The Journal of Neuroscience, June 15, 1998, *18*(12):4705–4721

Innervation of Histaminergic Tuberomammillary Neurons by GABAergic and Galaninergic Neurons in the Ventrolateral Preoptic Nucleus of the Rat

Jonathan E. Sherin,[1,2] **Joel K. Elmquist,**[1] **Fernando Torrealba,**[1,3] **and Clifford B. Saper**[1]

[1]*Department of Neurology and Program in Neuroscience, Beth Israel Deaconess Medical Center, Harvard Medical School, Boston, Massachusetts 02215,* [2]*Committee on Neurobiology, University of Chicago, Chicago, Illinois 60637, and* [3]*Facultad Ciencias Biologicas, Pontificia Universidad Catolica de Chile, Santiago 22, Chile*

The tuberomammillary nucleus (TMN) is the major source of histaminergic innervation of the mammalian brain and is thought to play a major role in regulating wake–sleep states. We recently found that sleep-active neurons in the ventrolateral preoptic nucleus (VLPO) provide a major input to the TMN, but the specificity of this projection and the neurotransmitters involved remain unknown. In this study, we examined the relationship of VLPO efferents to the TMN using both retrograde and anterograde tracing, combined with immunocytochemistry. We found that the descending projection from the VLPO selectively targets the cell bodies and proximal dendrites of the histaminergic TMN. In addition, VLPO axons could be traced into the brainstem, where they provided terminals in the the serotoninergic dorsal and median raphe nuclei, and the core of the noradrenergic locus coeruleus. Approximately 80% of the VLPO neurons that were retrogradely labeled by tracer injections including the TMN were immunoreactive either for galanin or for glutamic acid decarboxylase (GAD), the synthetic enzyme for GABA. Virtually all of the galaninergic neurons in the VLPO were also GAD positive. Our results indicate that the VLPO may provide inhibitory GABAergic and galaninergic inputs to the cell bodies and proximal dendrites of the TMN and other components of the ascending monoaminergic arousal system. Because these cell groups are simultaneously inhibited during sleep, the VLPO sleep-active neurons may play a key role in silencing the ascending monoaminergic arousal system during sleep.

Key words: sleep; arousal; basal forebrain; preoptic area; posterior hypothalamus; histamine

The tuberomammillary nucleus (TMN), located in the caudolateral hypothalamus, is the sole source of histaminergic innervation of the mammalian CNS (Snyder et al., 1974; Wilcox and Seybold, 1982; Watanabe et al., 1983, 1984; Wouterloud et al., 1986). Histaminergic output from the TMN is thought to play an important role in mediating forebrain arousal (Lin et al., 1986, 1988, 1990, 1994, 1996; Schwartz et al., 1991; Wada et al., 1991; Monti, 1993). For example, pharmacological augmentation of histaminergic transmission produces arousal (Monnier et al., 1970; Kalivas, 1982; Lin et al., 1990, 1994, 1996; Monti et al., 1991). Conversely, sleep is promoted by pharmacological blockade of central histaminergic receptors (Kiyono et al., 1985; Nicholson et al., 1985; Monti et al., 1986; White and Rhumbold, 1988; Tasaka et al., 1989), inhibition of histamine synthetic enzymes (Kiyono et al., 1985; Lin et al., 1988; Monti et al., 1988; Itowi et al., 1991), lesions of the TMN region (Lindsley et al., 1949; Swett and Hobson, 1968; Sallanon et al., 1988), or hyperpolarization of the TMN area with GABAergic agonists (Lin et al., 1989; Sallanon et al., 1989). TMN neurons demonstrate maximal rates of firing (and presumably transmitter release) during arousal, whereas firing decreases during slow wave sleep and virtually ceases during REM sleep (Vanni-Mercier et al., 1984; Steininger et al., 1996). The slowing of TMN firing during sleep is accompanied by an increase in GABA release in the TMN region (Nitz and Siegel, 1996).

Electron microscopic studies have demonstrated synapses onto TMN neurons by axon terminals that are immunoreactive for GABA or galanin (Kohler et al., 1986; Ericson et al., 1991b). Because both GABA and galanin inhibit monoaminergic neurons (Sundstrom and Melander, 1988; Seutin et al., 1989; Schonrock et al., 1991; Yang and Hatton, 1994; Pieribone et al., 1995), it would be important to know the sources of these inputs to the TMN cell bodies, which might play an important role in regulating wakefulness. Unfortunately, earlier studies of afferents to the TMN were able to identify only a few sources of sparse inputs to its cell-dense core (Wouterloud et al., 1987, 1988; Wouterloud and Gaykema, 1988; Ericson et al., 1991a; Wouterloud and Tuinhof, 1992).

Recently, we identified a group of neurons in the ventrolateral preoptic area (VLPO) that are retrogradely labeled by injections of retrograde tracers into the TMN (Sherin et al., 1996). VLPO neurons demonstrate Fos protein accumulation, suggesting that they are especially active specifically during sleep. Both GABAergic and galaninergic neurons are found clustered in the region of the VLPO (Mugnaini and Oertl, 1985; Melander et al., 1986), suggesting that VLPO neurons may inhibit the histaminergic TMN neurons during sleep. However, the terminal distribution of the descending projection from the VLPO to the TMN is not known, nor have the neurotransmitters in the pathway been identified. We therefore combined anterograde and retrograde tracing methods with immunocytochemistry for several putative neurotransmitters involved in this projection and its targets to

Received Dec. 4, 1997; revised March 2, 1998; accepted April 7, 1998.

Correspondence should be addressed to Dr. Clifford B. Saper, Department of Neurology, Beth Israel Deaconess Medical Center, 330 Brookline Avenue, Boston, MA 02215.

characterize the pathway from the VLPO to the TMN and its neurotransmitters.

MATERIALS AND METHODS

All experiments were performed on male Sprague Dawley rats weighing 250–350 gm and were performed using protocols that had been approved by the Harvard Medical School and Beth Israel Deaconess Medical Center Animal Care and Use Committees.

Retrograde tracer studies. Animals were anesthetized with chloral hydrate (350 mg/kg, i.p.) and placed in a stereotaxic apparatus, and a small burr hole was made above the posterolateral hypothalamus. Pressure injections of retrograde tracers were placed from a glass micropipette, using methods described previously (Herbert and Saper, 1990; Elmquist and Saper, 1996). Injections consisting of fast blue (Illing GmBH) (7.0% in saline, 10 nl; $n = 35$), diamido yellow (Illing GmBH) (7.0% in saline, 10 nl; $n = 3$), cholera-toxin B subunit (CTB) (List Biologic, Campbell, CA; 0.1% in saline, 1–5 nl; $n = 63$), or gold-conjugated CTB (List Biologic; 50.0% in saline, 3–9 nl; $n = 20$) were placed into the caudolateral hypothalamus at coordinates approximating the largest cluster of histaminergic neurons, the ventral TMN (TMNv) [anteroposterior (AP), −4.2; dorsoventral (DV), −9.1; left-right (LR), ± 1.35; in the flat skull position].

In another group of animals, extracellular recording was used to guide iontophoretic deposits of Fluorogold (Fluorochrome; 1.0% in sodium acetate buffer, pH 3.3, with 1 μA positive current, 7 sec on/7 sec off for 1 min; $n = 21$), which were placed through micropipettes using methods similar to those described previously (Aston-Jones et al., 1986; Pieribone and Aston-Jones, 1988). In brief, pipettes with tip diameters of 1–5 μm were positioned stereotaxically to the vicinity of the TMNv. Extracellular single unit and multiunit activity were then recorded using standard methods, and TMN neurons were identified as described previously (Reiner and McGeer, 1987). Injections of Fluorogold were placed specifically at these sites.

Animals were reanesthetized 8–10 d later and perfused with 50 ml saline (0.9%) followed by 500 ml formalin (10% in phosphate buffer, pH 7.0). Subsets of the animals that received injections of gold-conjugated CTB ($n = 20$) or fluorescent tracers ($n = 23$) received intracerebroventricular injections of colchicine (10 mg/ml in saline; 6 μl in each lateral ventricle) under chloral hydrate anesthesia 36–40 hr before they were killed to optimize immunocytochemical visualization (Moga and Saper, 1994; Herbert and Saper, 1990). Brains were removed, post-fixed for 4 hr in the same fixative, and then equilibrated in 20% sucrose in PBS (0.1 M; 0.9%, pH 7.0). Entire brains were sectioned (40 μm; one in four series) on a freezing microtome, and sections were stored at 4°C in tissue culture wells in PBS with sodium azide (0.02%) until they were used. Immunocytochemical procedures were used to detect CTB (Ericson et al., 1991a; Elmquist and Saper, 1996), whereas gold-conjugated CTB was detected using a commercially available silver intensification kit (Amersham, Arlington Heights, IL; Intense BL) (Llewellyn-Smith et al., 1990).

Anterograde tracing. Anterograde tracer experiments were drawn from a large series of cases ($n = 189$) of injections into the preoptic area and adjacent basal forebrain; VLPO injections had coordinates at approximately AP −0.45, DV −8.5, LR ±1.0. Injections of the anterograde tracer biotinylated dextran were made using methods that were essentially the same as the placement of retrograde tracer injections. Tracer was expelled by iontophoresis (Molecular Probes, Eugene, OR) (25% in dH_20 with 4 μA positive current, 7 sec on/7 sec off, for 10–20 min; $n = 44$) or an air pressure delivery system (12.5% in saline, 0.5–3.0 nl; $n = 145$). Animals were reanesthetized 5–10 d later and perfused, and the brains were sectioned, as in the retrograde transport experiments.

Biotinylated dextrans were visualized in one series of sections by incubation in peroxidase-conjugated avidin (Vector Elite ABC kit, 1:500; Vector Laboratories, Burlingame, CA) for 1 hr, followed by a 3,3 diaminobenzidine solution (DAB; 0.05%) containing hydrogen peroxide (0.01%). After sections were mounted on gelatin-coated slides, dehydrated in graded alcohols, and cleared in xylene, the DAB reaction product was intensified using a silver–gold intensification procedure, and sections were Giemsa-counterstained (de Lacalle et al., 1994). A second series of sections from several of these brains was prepared similarly for biotinylated dextran visualization to examine the relationship of labeled VLPO terminals with immunolabeled cell bodies and dendrites of potentially recipient neurons. Sections for this series were first incubated in peroxidase-conjugated avidin, as before, but stained blue-black (DAB and 0.01% cobalt chloride). Selected sections were then immunocytochemically stained brown (DAB alone) for various chemical markers (see below) found in neurons providing ascending projections associated with diffuse cortical or thalamic innervation that are thought to be associated with arousal or behavioral state control (Hallenger et al., 1987; Saper, 1987; Steriade, 1988; Steriade et al., 1993).

Immunocytochemistry. To identify CTB retrogradely labeled neurons, we used an antiserum raised against CTB (List Biologic) (goat, 1:100,000). To determine whether retrogradely labeled VLPO neurons contained GABA or galanin, we used antisera against glutamic acid decarboxylase (GAD) (Chemicon, Temecula, CA; rabbit, 1:10,000) (Gritti et al., 1994) and galanin (Peninsula Labs; rabbit, 1:10,000) (Elmquist et al., 1992). We used previously characterized antisera directed against choline acetyltransferase (gift of Dr. Lou Hersh, University of Kentucky; rabbit, 1:10,000) to demarcate cholinergic neurons in the diagonal band, pedunculopontine, and laterodorsal tegmental nuclei (de Lacalle, 1994); melanin-concentrating hormone (gift of Dr.Terri Maratos-Flier, Harvard Medical School; rabbit, 1:10,000) to demarcate cortically projecting tuberal lateral hypothalamic neurons (Saper et al., 1986; Bittencourt et al., 1992); adenosine deaminase (gift of Rodney Kellems, Baylor College of Medicine; sheep, 1:30,000) to demarcate histaminergic TMN neurons (Senba et al., 1985); tyrosine hydroxylase (Eugene Tech; rabbit, 1:10,000) to demarcate dopaminergic ventral tegmental area, substantia nigra, and noradrenergic locus coeruleus neurons); and serotonin (Incstar; rabbit, 1:10,000) to demarcate serotoninergic dorsal and median raphe neurons. For all immunocytochemical procedures, sections were kept at room temperature under gentle agitation in reagents diluted in PBS (0.1 M phosphate buffer, 0.9% NaCl, pH 7.0). Repeated washes between steps were performed in PBS. Sodium azide (0.025%), normal donkey serum (3.0%), and Triton X-100 (0.25%) were added to all incubations in antisera. Sections were incubated at room temperature in primary antiserum overnight (12–16 hr) and in biotinylated secondary antiserum (Jackson ImmunoResearch, West Grove, PA; donkey, 1:1000) for 1 hr. After incubation in secondary antiserum, sections were incubated in Cy3-conjugated avidin (Jackson ImmunoResearch; 1:250) for fluorescence visualization or in peroxidase-conjugated avidin (Vector Elite Kit; 1:500 in PBS) for bright-field visualization of immunoreactivity (ir) for 1 hr followed by DAB (0.05%) with hydrogen peroxide (0.01%). All sections were mounted onto gelatin-coated slides, dehydrated in graded ethanols, placed into xylenes, and coverslipped with Permaslip.

In addition, preoptic sections from several colchicine-treated animals were stained sequentially, using double-labeling immunofluorescence techniques, for both GAD-ir and galanin-ir. For these procedures, GAD-ir was visualized using a secondary antiserum that was directly conjugated to Cy-3 (Jackson ImmunoResearch; 1:250), and galanin-ir was visualized using a biotinylated secondary antiserum and FITC-conjugated avidin (Jackson ImmunoResearch; 1:250). Sequential stains were conducted in both directions (GAD and then galanin in one series, galanin and then GAD in another series). All sections were mounted on gelatinized slides, air-dried, washed in distilled water, dehydrated in alcohols of ascending concentration, put into xylenes overnight, and then coverslipped with Permount.

Immunocytochemical controls. For single-label controls, preoptic sections were incubated in GAD or galanin antisera that were preabsorbed with their respective antigens (50 μg/ml diluted serum). For double-label controls, because both primary antisera were raised in rabbits, preoptic sections were stained sequentially but with the second primary antiserum omitted or replaced with normal rabbit serum.

Electron microscopy. Sections from two rats with injections of biotinylated dextran into the preoptic area were prepared for electron microscopy. These animals were prepared as above, except that they were perfused with 2% paraformaldehyde–2.5% glutaraldehyde in 0.1 M PB, pH 7.4. Fifty micrometer sections were cut through the posterior hypothalamus using a vibrating microtome. Processing for biotinylated dextrans was as above, except that Triton X-100 was omitted. Sections were trimmed down to the TMN region, post-fixed in 1% osmium tetroxide, dehydrated in ethanol, and flat-embedded in Durcopan ACM (Fluka, Buchs, Switzerland) between a glass slide coated with Teflon spray (Polysciences, Warrington, PA) and a plastic coverslip. The block was trimmed further, and silver–gold thin sections were cut on an ultramicrotome and picked up on nickel grids for post-embedding immunocytochemistry to reveal GABA-ir. Thin sections were incubated in rabbit anti-GABA antibodies (Incstar) at 1:300 dilution for 24 hr at room temperature and then in a goat anti-rabbit secondary antiserum conjugated to 10 nm gold colloid gold particles, at 1:15 dilution for 2 hr at 37°C. After post-fixation in 2% glutaraldehyde in cacodylate buffer for 10 min

and subsequent rinses in buffer, the sections were counterstained with uranyl acetate and lead citrate. The specificity of the primary antibody was tested by omission or by preincubation with 10 mM GABA. In both cases, no immunolabeling was observed.

Data analysis. Series processed for fluorescence microscopy were viewed through UV (for fluorogold, fast blue, and diamido yellow), rhodamine (for ADA-ir, GAD-ir, galanin-ir), and FITC (for galanin-ir in double-stained tissue) filter cubes (Leica, Nussloch, Germany). Series processed for light-microscopy were viewed under bright- or dark-field illumination. The precise location of each retrograde tracer injection site with respect to the TMN was determined by examining its relationship to ADA-ir cell bodies that, at the ventrolateral surface of the caudolateral hypothalamus, specifically demarcate the core of the TMNv (Senba et al., 1985). Analysis of retrograde tracer data involved correlating patterns of retrograde label throughout the brain with injection sites that were either confined to the core of the TMNv, included the core of the TMNv and adjacent structures, or were adjacent to but did not include the core of the TMNv. Immunostained preoptic sections from colchicine-pretreated animals that received injections of retrograde tracer that included the core of the TMNv were inspected for VLPO neurons containing retrograde label and GAD-ir or galanin-ir. The percentage of retrogradely labeled VLPO neurons that were immunolabeled for GAD or galanin was then calculated. Double-immunostained sections containing the VLPO from colchicine-pretreated animals were inspected for both GAD-ir and galanin-ir to determine whether these markers were present in the same neurons.

Giemsa-counterstained sections from anterograde tracer cases were analyzed under both dark- and bright-field illumination to determine the relationship between cell groups included in injection sites in the VLPO region and resultant fiber connections throughout the brain. The injection sites were plotted onto drawings of Giemsa-stained sections through the preoptic area that were used as a reference. The course of fibers emanating from injection sites were plotted using a camera lucida apparatus. Double-stained sections were analyzed under high-power bright-field illumination to determine the relationships between immunostained cell bodies and dendrites (brown) and fibers originating in the VLPO (blue-black).

Electron microscopic material was examined for both GABA-immunoreactive and biotinylated dextran-labeled axon terminals making contacts with TMN neurons. Dense intracellular precipitate marked anterogradely labeled terminals. GABA-immunoreactivity was determined by measuring the density of colloid-gold particles over axon terminals and postsynaptic structures. There was a clear bimodal distribution of level of labeling. One group of structures had labeling similar to background (0–5 particles/μm^2) and was considered unlabeled. A second group of structures with labeling of greater than 10 particles/μm^2 was considered to be labeled.

Photography. Bright-field photomicrographs were produced by capturing images with a digital camera (Kodak DCS 460) mounted directly on the microscope. Fluorescence photomicrographs were photographed on color slide film (Kodak, Ektachrome 400), and slides were converted to digital images (Nikon, Coolscan). Image-editing software (Adobe Photoshop version 3.0) was used to combine photographs and to create montages from different focal planes of the same field. Contrast, brightness, and sharpness were adjusted, and figures were printed by a dye sublimation printer (Kodak 8600).

RESULTS

Cytoarchitecture

We adopted a nomenclature for the preoptic area that synthesizes our own data with that of a large body of literature (Simerly et al., 1984; Simerly, 1995). Although the VLPO is difficult to demarcate on cytoarchitectonic grounds alone, it may be distinguished in coronal sections as a small, roughly triangular-shaped cell group, with its base along the flat surface of the brain between the optic chiasm and the diagonal band. Its neurons are wedged along the medial aspect of the horizontal limb of nucleus of the diagonal band, and they are often separated from it by a small penetrating blood vessel (Fig. 1*a*, Table 1). The VLPO is most prominent in the caudal half of the preoptic area and is found dorsal and lateral to the rostral pole of the supraoptic nucleus. It extends caudally to about the level of the rostral pole of the suprachiasmatic nucleus. The VLPO can be most easily delineated with markers for Fos-ir after periods of sleep (Sherin et al., 1996) (Fig. 1*b*) or galanin-immunoreactivity in colchicine-pretreated animals (Melander et al., 1986) (Fig. 1*c*).

For the TMN we use the terminology of Ericson et al. (1987) who recognized the major cluster of histaminergic neurons in the TMNv as well as a smaller cluster medially (TMNm) and a diffuse collection of cells (TMNd) in between. However, we considered the rostral and caudal extensions of the TMN to be part of the TMNv rather than separate tuberal and caudal magnocellular nuclei (Bleier et al., 1979).

Retrograde tracing studies

The relationship of injection sites to the TMN was most easily appreciated in the cases that involved the TMNv. In most cases the injection site also involved various amounts of surrounding tissue. However, in one case, J-13, a small injection of Fluorogold placed by electrophysiological guidance was tightly confined to the cell-dense core of the TMNv as demonstrated in sections that were counterstained for adenosine deaminase-ir (Fig. 2*a,b*). In this case, the vast majority of retrogradely labeled neurons was concentrated in a longitudinal column, roughly 0.4 mm long, which extended rostrocaudally along the ventral-most portion of the lateral preoptic area (VLPO) (Fig. 2). Smaller numbers of individual, retrogradely labeled neurons streamed dorsally and medially from this column into adjacent cell groups in the preoptic area and were scattered diffusely in the lateral septum, the bed nucleus of the stria terminalis, the substantia innominata, and the horizontal limb of the diagonal band nucleus (Fig. 2*c*). No retrogradely labeled neurons were identified in other forebrain or brainstem cell groups after this injection.

The pattern of retrograde labeling seen in case J-13 was found in 49 additional cases in which the injection site included the core of the TMNv (e.g., see *J-39* in Fig. 3). However, because these cases also included regions surrounding the TMN, a more widespread pattern of retrograde labeling was observed, as reported previously by Ericson et al. (1991a). Nevertheless, the amount of retrograde labeling in the VLPO consistently corresponded with the degree to which the core of the TMNv was involved by retrograde tracer injection.

In 52 cases in which injection of retrograde tracer involved structures adjacent to but not including the core of the TMNv (see *J-9* and *J-10* in Fig. 3), retrogradely labeled cells were essentially absent from the VLPO but were found concentrated in adjacent preoptic and basal forebrain cell groups. Other than the VLPO projection to the core of the TMN, we found no consistent differences in patterns of retrograde labeling between the cases that included TMN in the injection site and those that did not. Hence, although it can be concluded that the VLPO is a major source of afferents to the TMN, these experiments cannot rule out the possibility that smaller numbers of afferents to the core of the TMNv arise from adjacent parts of the preoptic area and basal forebrain.

Anterograde tracer studies

To better define the sources and terminal distributions of inputs from the preoptic area to the TMN, we examined cases drawn from a large series of 189 experiments in which the projections of the preoptic area and surrounding basal forebrain were systematically explored with small injections of the anterograde tracer biotinylated dextran. In 12 of these cases, the injection sites involved the VLPO to varying degrees (for summary of injection

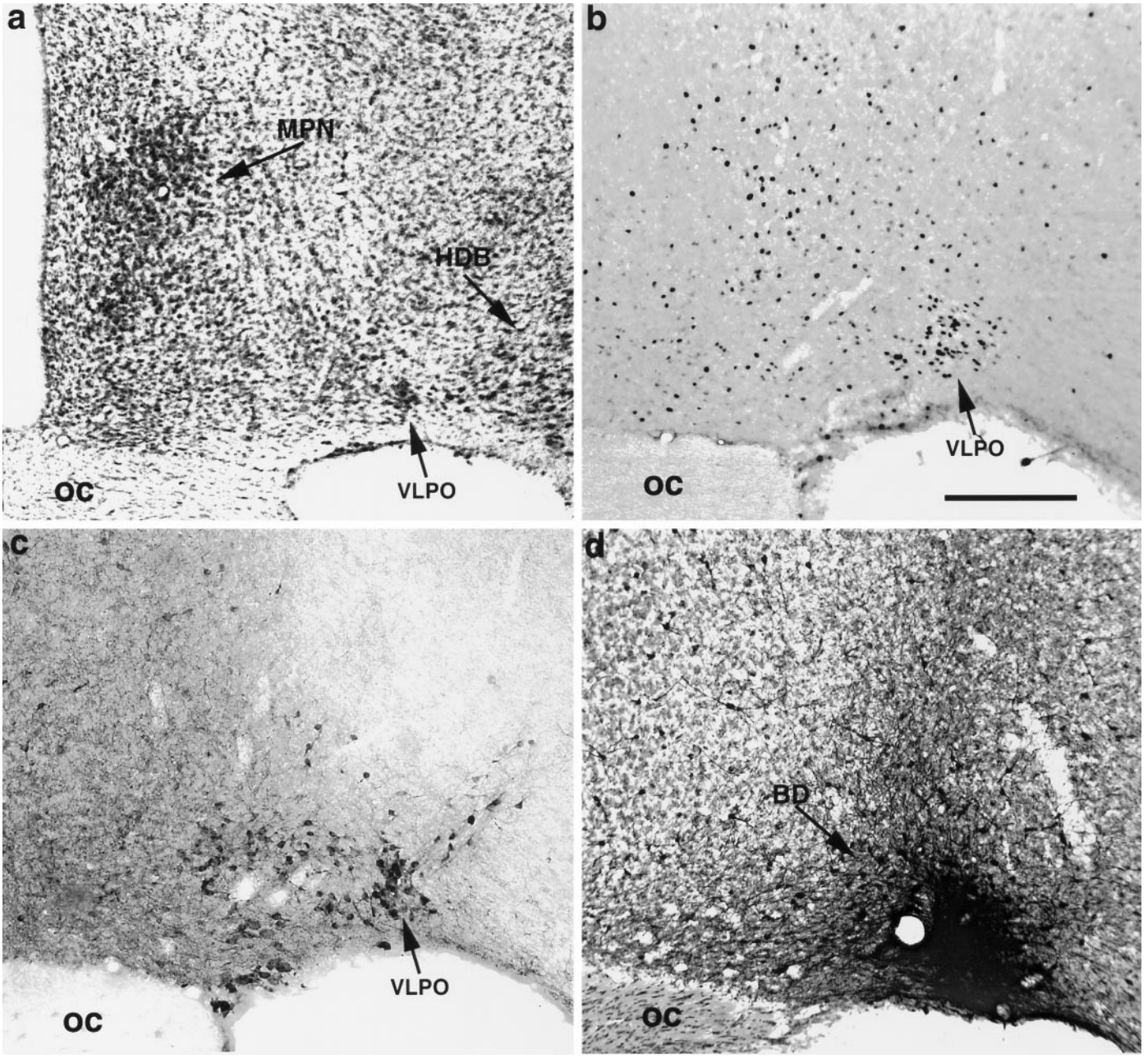

Figure 1. A series of bright-field photomicrographs illustrating various histological markers for identifying the ventrolateral preoptic nucleus. *a* shows the appearance of the VLPO in Giemsa-stained sections as a small triangular cluster of neurons along the ventral surface of the brain, with its lateral edge bordering the nucleus of the horizontal limb of the diagonal band. *b* illustrates the Fos-immunoreactive neuronal nuclei in the VLPO after a 1 hr period spent predominantly asleep. In *c*, the VLPO is clearly demarcated as a galanin-immunoreactive cell group in a colchicine-pretreated animal. *d* shows an injection site of biotinylated dextran (*BD*) in case VLPO 11; the section is counterstained with Giemsa. The borders of the injection site correspond closely with the location of the cluster of Fos-positive and galanin-positive neurons seen in *b* and *c*. Scale bar (shown in *b*): *a*, 500 μm; *b–d*, 300 μm.

sites, see Fig. 4). In each of three cases (VLPO 11, VLPO 38, R 1059) the injection site was largely confined to the VLPO. Experiment VLPO 11 best demonstrated the full pattern of efferent projections from this cell group (Fig. 5a). This relatively large iontophoretic injection essentially filled the VLPO, with minimal spread into neighboring structures such as the supraoptic nucleus, the medial preoptic area, the dorsal lateral preoptic area, the diagonal band nucleus, or the anterior hypothalamic area (Fig. 1*d*). However, a few scattered neurons were retrogradely labeled in other preoptic cell groups as well as in the lateral septum and the bed nucleus of the stria terminalis.

In case VLPO 11, labeled fibers left the injection site ipsilaterally through medial (periventricular), dorsal (stria medullaris), and lateral (medial forebrain bundle) pathways. Minor contralateral projections were found to cross in the ventral supraoptic commissure and provide similarly distributed projections to the contralateral side of the brain. Fibers that ascended into the telencephalon ramified throughout the basal forebrain and septal-

Table 1. Abbreviations used in figures

3	Oculomotor nucleus
3V	Third ventricle
4V	Fourth ventricle
5	Trigeminal nucleus (motor division)
6	Abducens nucleus
7n	Facial nerve (g, genu)
12	Hypoglossal nucleus
ac	Anterior commissure
ACB	Nucleus accumbens
AHN	Anterior hypothalamic nucleus
AM	Anteromedial thalamic nucleus
Amb	Nucleus ambiguus
APFX	Anterior perifornical nucleus
ARC	Arcuate nucleus
AV	Anteroventral thalamic nucleus
AVPV	Anteroventral preoptic nucleus
bc	Brachium conjunctivum
BD	Biotinylated dextran injection site
BNST	Bed nucleus of the stria terminalis
CA	Cerebral aqueduct
Cb	Cerebellum
cc	Corpus collosum
CM	Centromedial thalamic nucleus
cp	Cerebral peduncle
CPu	Caudate-putamen
cst	Corticospinal tract
DB	Diagonal band nucleus
DMH	Dorsomedial hypothalamic nucleus
DT	Dorsal tegmental nucleus
EP	Entopeduncular nucleus
fr	Fasciculus retroflexus
fx	Fornix
GP	Globus pallidus
HDB	Horizontal limb of the diagonal band nucleus
ic	Internal capsule
IO	Inferior olive
IP	Interpeduncular nucleus
LC	Locus coeruleus
LDT	Laterodorsal tegmental nucleus
LH	Lateral habenular nucleus
LS	Lateral septal nucleus
LSV	Ventral lateral septal nucleus
LV	Lateral ventricle
MCPO	Magnocellular preoptic nucleus
MD	Mediodorsal thalamic nucleus
Me5	Mesencephalic trigeminal nucleus
MH	Medial habenular nucleus
ml	Medial lemniscus
MLF	Medial longitudinal fasciculus
MM	Medial mammillary nucleus
MnPO	Median preoptic nucleus
MPB	Medial parabrachial nucleus
MPN	Medial preoptic nucleus
MR	Median raphe nucleus
mt	Mammillothalamic tract
NLOT	Nucleus of the lateral olfactory tract
NST	Nucleus of the solitary tract
NTB	Nucleus of the trapezoid body
oc	Optic chiasm
ot	Optic tract
OVLT	Organum vasculosum of the lamina terminalis
PAG	Periaqueductal gray matter
pc	Posterior commissure
PF	Parafascicular nucleus
PHA	Posterior hypothalamic area
PMD	Dorsal premammillary nucleus
PMV	Ventral premammillary nucleus
Pn	Pontine nuclei
Pr5	Principal sensory trigeminal nucleus
PTA	Pretectal area
PVH,r	Paraventricular hypothalamic nucleus, rostral pole
PVT	Paraventricular thalamic nucleus
py	Pyramidal tract
Re	Reuniens thalamic nucleus
RM	Raphe magnus nucleus
RN	Red nucleus
RP	Raphe pontis nucleus
Rpa	Raphe pallidus nucleus
RPT	Reticular tegmental nucleus of the pons
RT	Reticular thalamic nucleus
SCN,r	Suprachiasmatic nucleus, rostral pole
SFO	Subfornical organ
SHy	Septohypothalamic nucleus
sm	Stria medullaris
SNc,r	Substantia nigra, pars compacta, pars reticulata
SO	Superior olivary complex
SON,r	Supraoptic nucleus, rostral pole
Sp 5	Spinal trigeminal nucleus
sp5	Spinal trigeminal tract
SUM	Supramammillary nucleus
tb	Trapezoid body
TMNm,v	Tuberomammillary nucleus, medial and ventral parts
VA	Ventral anterior thalamic nucleus
VB	Ventrobasal thalamic complex
VDB	Vertical limb of the diagonal band nucleus
VLL	Ventral nucleus of the lateral lemniscus
VL	Ventral lateral thalamic nucleus
VLM	Ventrolateral medulla
VLPO	Ventrolateral preoptic nucleus
VMH	Ventromedial hypothalamic nucleus
VMPO	Ventromedial preoptic nucleus
VTA	Ventral tegmental area
VTN	Ventral tegmental nucleus (of Gudden)
ZI	Zona incerta

diagonal band complex. Ascending and local fibers within the diencephalon infiltrated most preoptic structures, particularly the ventromedial preoptic area and the median preoptic nucleus (Elmquist and Saper, 1996; Elmquist et al., 1996). Very little input was seen to the suprachiasmatic nucleus. Descending fibers (which constitute the largest contingent of fibers produced by injection of tracer into the VLPO) traversed the hypothalamus in the medial forebrain bundle and targeted many anterior, lateral, and posterior hypothalamic nuclei. Particularly intense hypothalamic innervation was seen in the perifornical area, the tuberal lateral hypothalamic area, the parvocellular parts of the paraventricular nucleus, the supramammillary region, and all divisions of

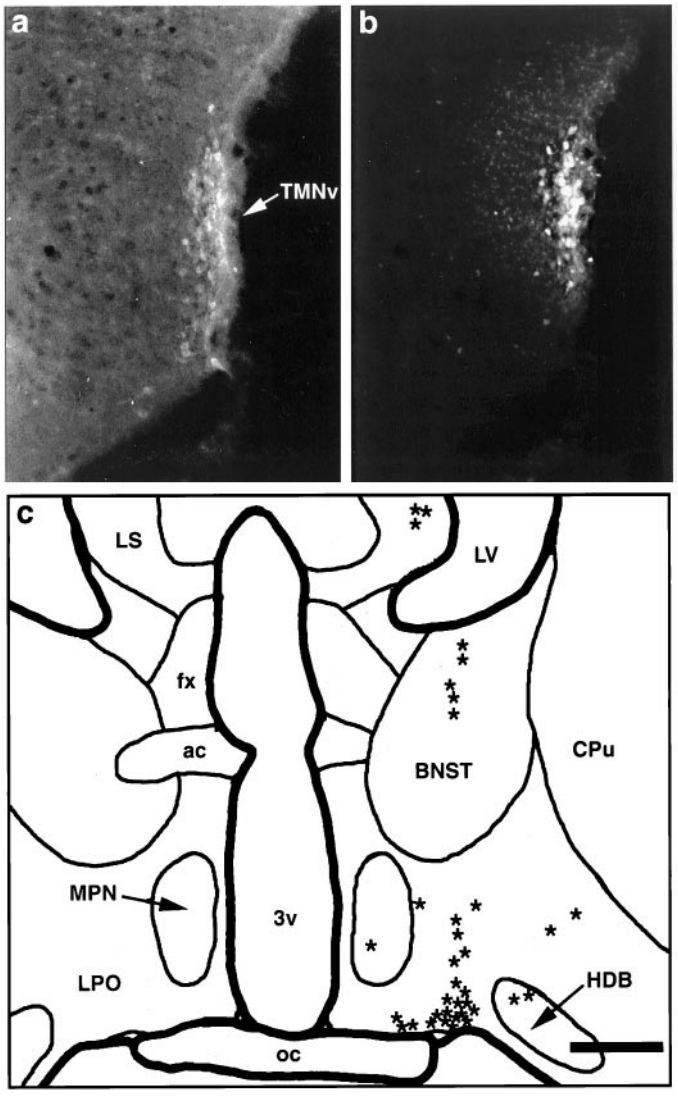

Figure 2. Summary of findings from a fluorogold injection into the core of the TMNv with no involvement of adjacent structures. *a*, Fluorescence photomicrograph of a caudal hypothalamic section stained immunocytochemically for adenosine deaminase, as visualized using a rhodamine filter cube. Immunoreactive neurons delineate the TMNv (*arrow*). *b*, Fluorescence photomicrograph of the same field, demonstrating Fluorogold fluorescence as seen through a UV filter cube, showing that the center of the injection is limited to and essentially demarcates the TMNv. *c*, Camera lucida drawing of a caudal preoptic section showing retrogradely labeled cells (each *asterisk* represents one cell) produced by the injection in *b*. In this case, the vast majority of retrogradely labeled neurons were concentrated in the ventral portion of the lateral preoptic area. This pattern of labeling extended roughly 300 μm rostrally and 100 μm caudally from the level drawn. Scale bar (shown in *c*): *a, b*, 400 μm; *c*, 800 μm.

the TMN (Fig. 5*f–j*). Most impressive was a dense plexus of fibers and terminals that engulfed the magnocellular neurons in the TMNv (Fig. 6*a,b*). Dense innervation was also seen in the lateral habenular nuclei, and light innervation was present in the intralaminar and midline thalamic cell groups.

Some of the labeled fibers in case VLPO 11 continued caudally into the brainstem through periventricular and medial forebrain bundle systems to provide innervation of the ventral tegmental area and the substantia nigra as well as the ventral and ventrolateral parts of the periaqueductal gray matter in the midbrain and pons (Fig. 5*k–m*). Each raphe cell group in the rostral brainstem was found to contain labeled fibers, with the dorsal, caudal linear, and median divisions receiving relatively dense terminal innervation (Fig. 5*k–n*). The lateral parabrachial nucleus and the pedunculopontine and laterodorsal tegmental nuclei were additionally innervated (Fig. 5*n,o*), and the core of the locus coeruleus (Fig. 5*o*) contained many labeled axons displaying terminal boutons. Labeled fibers reached the medullary raphe nuclei as well as the ventromedial and ventrolateral medullary reticular formation where they provided terminal innervation (Fig. 5*p,q*), but no labeled axons could be followed into the spinal cord.

Two smaller injections that filled the VLPO less extensively (VLPO 38, R 1059) demonstrated a similar pattern of innervation, except for noticeable reductions in the relative intensity of labeling in the basal forebrain, the septal-diagonal band complex, the median preoptic nucleus, the anterior perifornical area, and the paraventricular hypothalamic nucleus. Within the caudal hypothalamus, efferents from these injections more selectively targeted the TMNv (avoiding adjacent cell groups), and provided input to the TMNm, TMNd, and supramammillary nucleus. Other injection sites that included the VLPO, but also included portions of neighboring cell groups ($n = 9$), confirmed the pattern of VLPO projections. In all cases that included the VLPO, there was dense terminal labeling in the TMNv as well as smaller numbers of labeled axons and terminals in the ventral tegmental area, the dorsal and median raphe nuclei, the pedunculopontine and laterodorsal tegmental nuclei, and the locus coeruleus.

Less intense but still substantial input to the TMN was seen in cases where the injection of biotinylated dextran was positioned in the lateral preoptic area dorsal to the VLPO. In these experiments, the labeled fibers descended more diffusely through the posterior lateral hypothalamus than after VLPO injections, providing a less specific input that also included structures immediately adjacent to the cell dense region of the TMN. Labeled axons in these cases were also traced into the brainstem through the periventricular and ventral tegmental fiber systems, and some labeled fibers were seen in the raphe nuclei, the pedunculopontine and laterodorsal tegmental nuclei, and the locus coeruleus, providing scattered axon terminals.

Control injections into cell groups that surround the VLPO, including the medial and lateral preoptic areas, the bed nucleus of the stria terminalis, and the lateral septal nucleus, produced patterns of labeling that were distinct from those cases with tracer injections into the VLPO. A detailed account of these patterns is beyond the scope of this report but our observations were consistent with earlier reports of projections from the septal-diagonal band complex (Meibach and Siegel, 1977; Swanson and Cowan, 1979), the preoptic area (Conrad and Pfaff, 1976; Swanson, 1976; Swanson et al., 1984; Chiba and Murata, 1985; Simerly and Swanson, 1988; Rivzi et al., 1995), the bed nucleus of the stria terminalis (Moga et al., 1989; Semba et al., 1989), the substantia innominata (Swanson et al., 1984; Tomimoto et al., 1987; Grove, 1988), and the anterior hypothalamic area (Saper et al., 1978; Risold et al., 1994). Only small numbers of labeled fibers were seen in the TMNv and TMNd after these injections, particularly those into the caudolateral septum, the caudal bed nucleus of the stria terminalis, the horizontal limb of the diagonal band nucleus, and the substantia innominata. In addition, medial preoptic sites demonstrated inputs of variable intensity to the TMNm and TMNd, with occasional inputs to the TMNv.

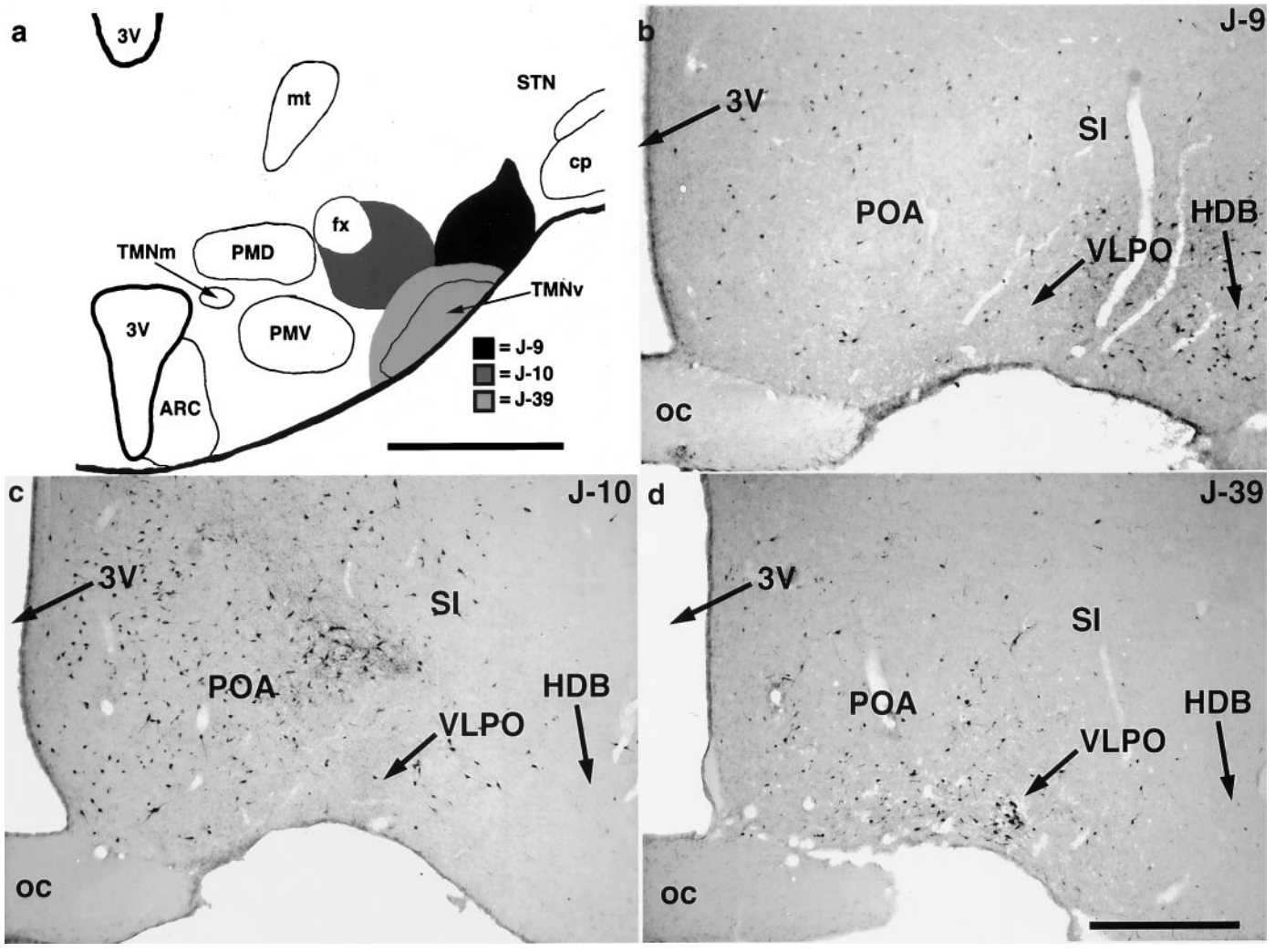

Figure 3. Summary of findings from three animals with CTB injections into the posterolateral hypothalamus demonstrating the topographical projections to this area from the preoptic area. *a*, Injection sites from these cases plotted onto a representative schematic of the TMNv in the caudal hypothalamus. *b–d*, Bright-field photomicrographs of preoptic sections at the level of the VLPO from these cases demonstrating the resultant pattern of retrograde label. Note that the VLPO contained a cluster of retrogradely labeled neurons after an injection that included the cell-dense core of the TMNv (*J-39*). However, few retrogradely labeled neurons were seen in the VLPO after injection of retrograde tracer into structures dorsomedially (*J-10*) or dorsolaterally (*J-9*) adjacent to the core of the TMNv. Scale bar, 700 μm.

Anterograde tracing of VLPO inputs to specific, chemically defined cell groups

The projections from the VLPO reach virtually all of the major cell groups, which provide diffuse ascending input to either the thalamus or cerebral cortex and which have been identified with the ascending arousal system (Saper, 1987). To better define the relationships of descending fibers from injections that were centered in the VLPO with individual, immunocytochemically identified neurons in these cell groups, we examined sections that had been double-stained for biotinylated dextran as well as various neurotransmitters or their synthetic enzymes that are contained in the diffuse ascending arousal pathways. In the nucleus of the diagonal band, for example, fiber labeling could be seen in close proximity to ChAT-like immunoreactive cell bodies and dendrites. However, appositions between labeled terminals and cholinergic cells were identified only rarely. Although similar overlap was observed in the pedunculopontine tegmental and laterodorsal tegmental nuclei, appositions between labeled fibers and individual ChAT-immunoreactive neurons were rare. In the tuberal lateral hypothalamic area, only rare appositions could be identified between labeled axons and melanin-concentrating hormone (MCH)-immunoreactive neurons.

In contrast, in caudal hypothalamic sections many appositions were observed between labeled fibers and TMN neurons identified by immunostaining for adenosine deaminase (Fig. 6*c*,*d*). [Adenosine deaminase is selectively found in histaminergic neurons in the TMN (Senba et al., 1985) and is used as a substitute marker because carbodiimide fixation for histamine is incompatible with anterograde tracing.] Repetitive appositions by single axons were seen along the cell bodies and proximal dendrites of recipient TMN neurons. In the core of the TMNv, where histaminergic neurons were tightly clustered, all focal planes were littered with numerous, labeled boutons interposed between adjacent immunopositive cell bodies.

In the brainstem, many labeled boutons were seen in the major monoaminergic cell groups, although the relationship of the la-

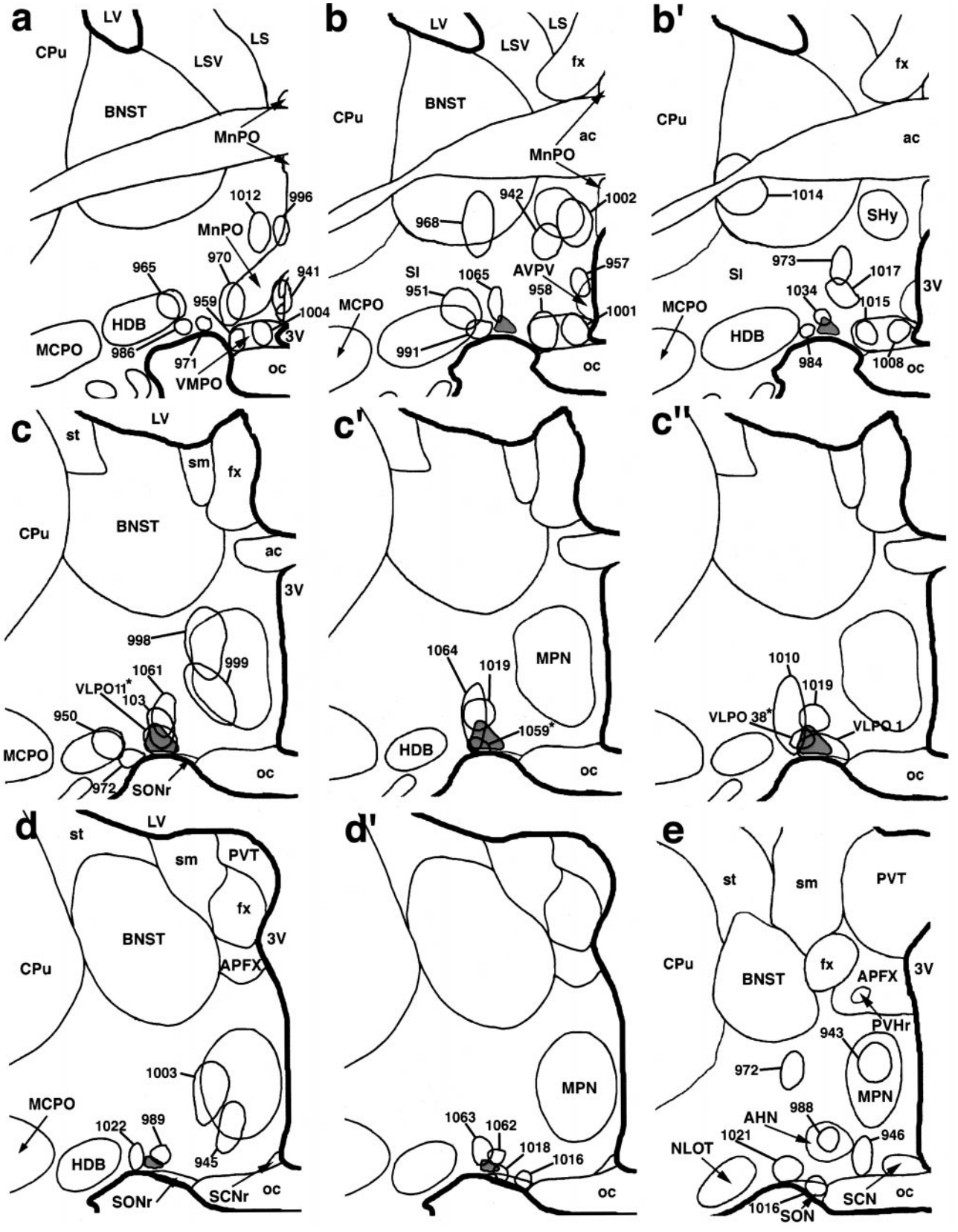

Figure 4. A summary diagram illustrating biotinylated dextran injection sites at six levels of the preoptic area. The VLPO is most prominent in schematics *c*, *c′*, *d*, and *d′* (in *light gray*). *Asterisks* denote cases VLPO 11, VLPO 38, and R 1059 in which biotinylated dextran injections were predominantly located within the VLPO (see Results).

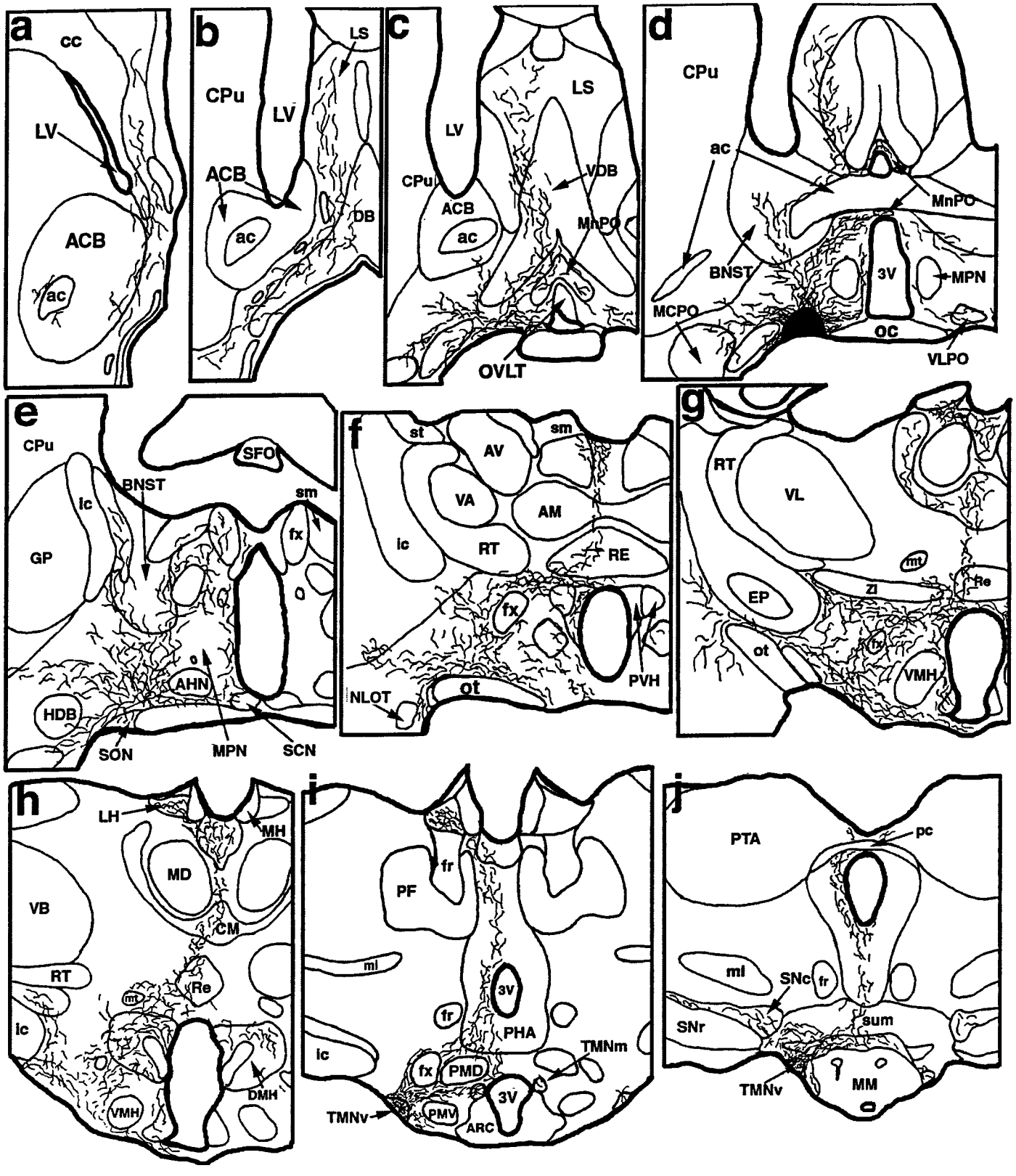

Figure 5. A series of camera lucida drawings illustrating the pattern of axonal labeling in case VLPO 11 (see Fig. 1 for photomicrograph of injection site). Note dense and selective innervation of all parts of the histaminergic tuberomammillary nucleus as well as the selectivity of innervation of the dopaminergic ventral tegmental area, serotoninergic dorsal, median, pontine, and medullary raphe nuclei, cholinergic pedunculopontine and laterodorsal tegmental nuclei, and noradrenergic locus coeruleus.

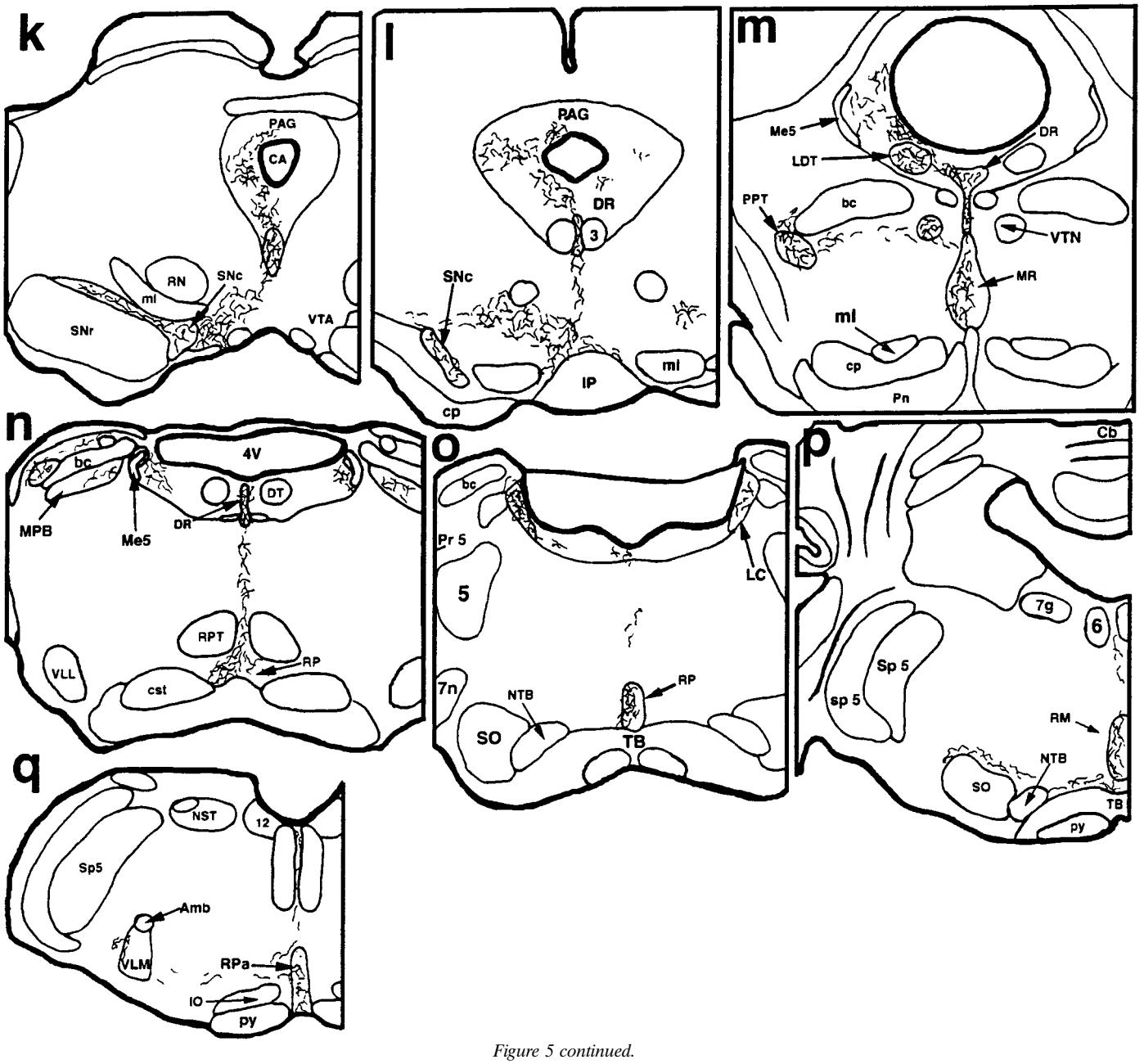

Figure 5 continued.

beled axons with specific cell types was less clear than in the TMN. In the ventral tegmental area, terminal-laden axons were found to course in the vicinity of TH-ir neurons, and in some of these instances, appositions were apparent. In the dorsal and median raphe nuclei, fibers from the VLPO overlapped closely with the distribution of serotonin-ir cell bodies and often displayed boutons in apposition with their cell bodies and large caliber dendrites. However, in both the dopaminergic and serotoninergic cell groups, many terminals did not have obvious relationships to immunostained cell bodies. In the relatively homogeneous noradrenergic locus coeruleus, fibers with boutons could be seen enmeshed between adjacent TH-immunoreactive cell bodies and apposing large immunoreactive dendrites throughout the entire rostrocaudal extent of its cell-dense core. However, these fibers were not nearly as numerous as those in the raphe nuclei or TMN.

Electron microscopy

To determine whether the anterogradely labeled axons made synaptic contacts with TMN neurons, sections from eight additional animals were examined ultrastructurally. In four cases in which the injection site included the VLPO, anterogradely labeled terminals, filled with cytoplasmic electron-dense reaction product that outlined mitochondria and synaptic vesicles, were abundant in the TMNv. Profiles of VLPO axon terminals were round or bilobed, typically containing one or more mitochondria, and densely packed with small, clear, round synaptic vesicles (Fig. 7). Dense-core vesicles were not seen. In one animal with optimal ultrastructural preservation, the labeled terminals were seen to make symmetric synaptic contacts with large dendritic profiles and, less often, with neuronal cell bodies or thin dendrites. The cell bodies were of the type described previously for TMN

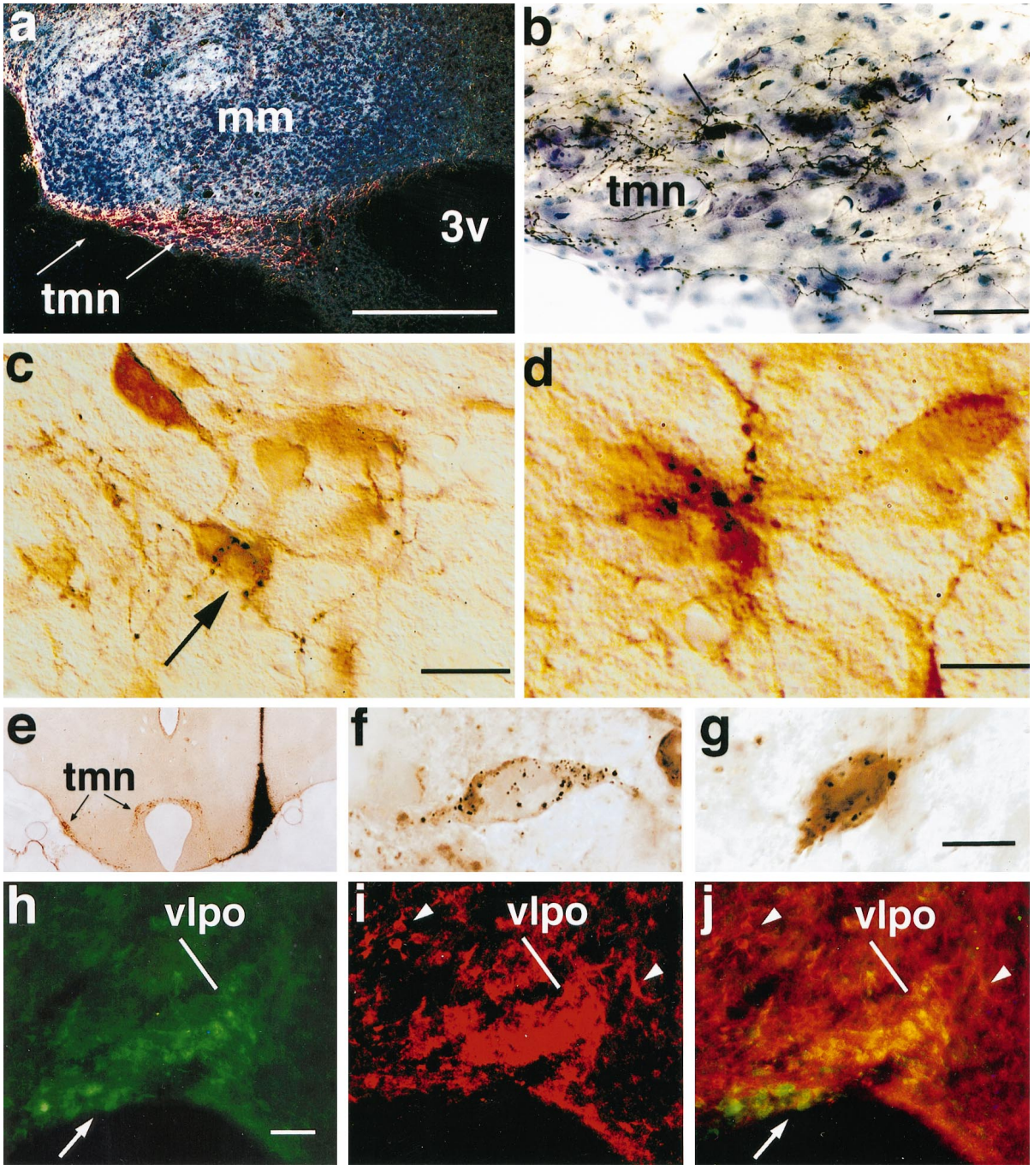

Figure 6. A series of photomicrographs to illustrate the innervation of the TMN histaminergic neurons by the VLPO. *a* shows a dark-field photomicrograph of anterogradely labeled VLPO axons in the TMN (indicated by *arrows*). The same area is shown at higher magnification in a bright-field photomicrograph in *b*, to demonstrate the large numbers of labeled axons and terminals. A single retrogradely labeled neuron (*arrow*) is seen in the TMN. *c* demonstrates the relationship of these axons to TMN cell bodies, in a different experiment in which the TMN neurons were stained immunocytochemically (*brown*) for adenosine deaminase. Individual *black axons* and terminals can be seen closely associated with immunoreactive cell bodies and dendrites (Nomarski optics). The neuron indicated by the *arrow* is illustrated at higher magnification and in a slightly different focal plane in *d*, receiving multiple appositions from a single axon. *e* shows a bright-field photomicrograph of a coronal section through the caudal hypothalamus demonstrating the center of an injection of gold-conjugated CTB in case J-78. This section was stained first for gold particles with a silver intensification procedure (*black*), followed by adenosine deaminase immunocytochemistry (*brown*) to identify histaminergic neurons. Note that the injection spreads dorsally above but manages to fill the rostral TMNv. This injection continues caudally into the heart of the TMNv. *f* and *g* show high-power bright-field Nomarski photomontages of VLPO neurons from case J-78, showing individual, retrogradely labeled neurons (*black* granular precipitate) that are GAD-immunoreactive (*brown*; *f*) or galanin-immunoreactive (*brown*; *g*). Photomontage was necessary to combine different focal planes to keep the CTB granules in focus. *h–j* illustrate the labeling of VLPO neurons with antisera against both galanin (*h*) and GAD (*i*). Note that because GAD antiserum also stains many axon terminals in the VLPO, this image is shown at much higher contrast to highlight the GAD-ir cell bodies, which appear as a cluster in the VLPO rather than as discrete cell bodies. Other GAD-positive cell bodies outside the VLPO are indicated by *arrowheads*. A double exposure in *j* demonstrates the double-labeled neurons in the VLPO as a *bright gold color*, whereas single-labeled neurons in the supraoptic nucleus (for galanin, *arrow*) and in the lateral preoptic area for (GAD, *arrowheads*) demonstrate that the antisera used do not cross-react. See Table 2. Scale bars: *a*, 250 μm; *b*, 50 μm; *c*, 25 μm; *d*, 10 μm; (shown in *g* for *e–g*): *e*, 650 μm; *f, g*, 20 μm; (shown in *h* for *h–j*): *h–j*, 100 μm.

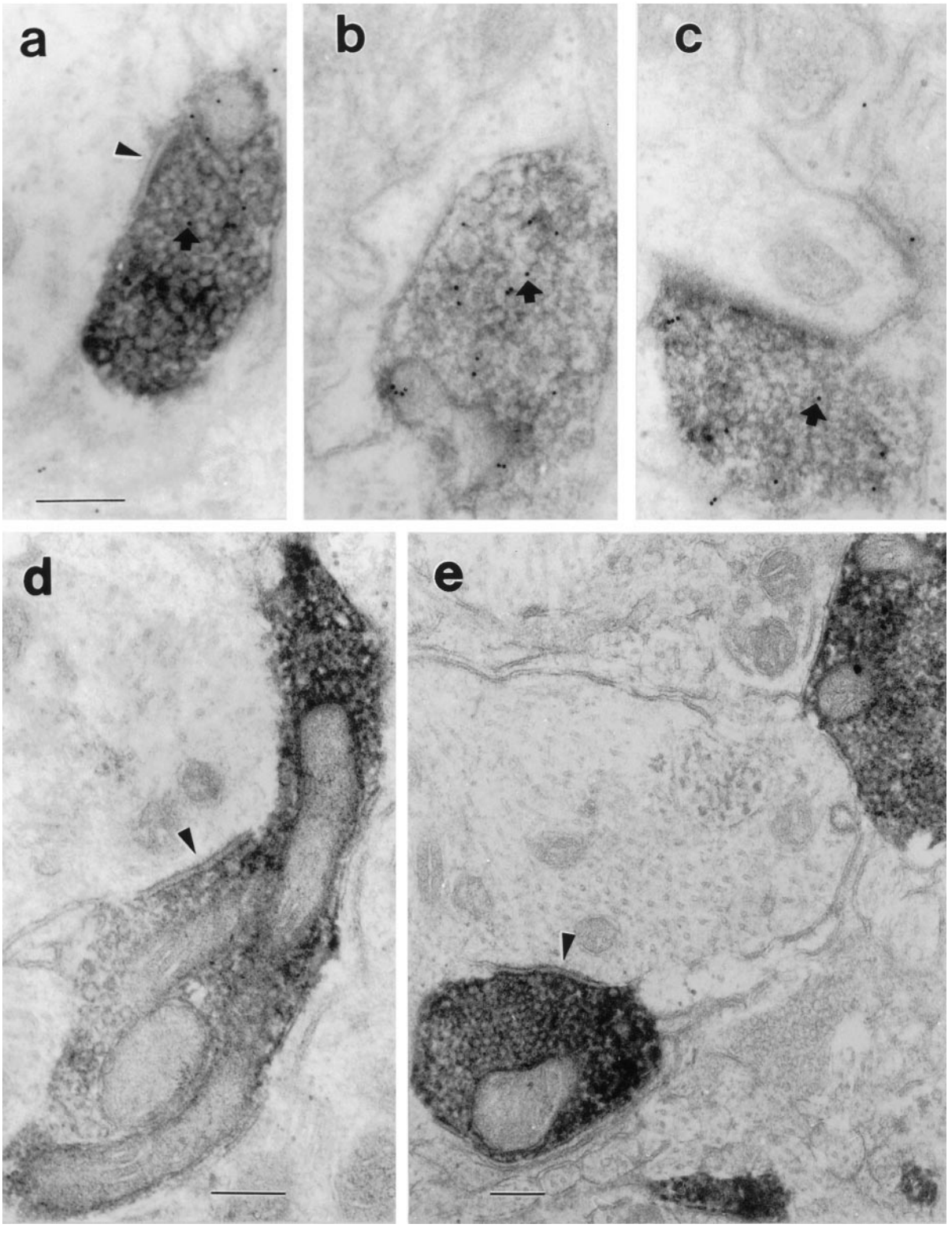

Figure 7. Electron micrographs illustrating the relationship of anterogradely labeled terminals from the VLPO with neurons within the TMN core. The anterograde label appears as an electron-dense precipitate filling axons and terminals but outlining mitochondria and vesicles. In *a–c*, the sections have been stained with a post-embedding immunocytochemical method, using 10 nm colloidal gold-labeled antibodies. Small, dark gold particles may be seen (*arrows*) over these terminals, which are therefore also GABA-immunoreactive. In *a*, *d*, and *e*, the labeled terminal makes a symmetric synapse with unlabeled large dendrites (*arrowheads*). Scale bar, 0.2 μm for all panels.

histaminergic neurons (Hayaishi et al., 1984; Ericson et al., 1987; Yamamoto et al., 1990). We observed no contacts with dendritic spines or axons.

The post-embedding immunogold technique revealed a bimodal distribution of immunolabeling of a random sample of axon terminals. About one-third (25 of 69) of unlabeled axon terminals were considered GABA-immunoreactive, with a mean of ~30 particles/μm^2. Gold particles over labeled terminals were typically associated with both vesicles and mitochondria, as has been described previously (Merighi and Polak, 1993). The remaining axon terminals, with 0–5 gold particles//μm^2, were judged to be GABA-negative. Virtually all of the anterogradely labeled VLPO terminals were in the clearly GABA-immunoreactive group. For a sample of 53 anterogradely labeled VLPO terminals, there was a mean of 20.09 gold particles/$\mu m^2 \pm$ 1.73 (SEM). Postsynaptic elements or other cell bodies or dendrites were never immunoreactive (mean of 1.56 ± 0.23 gold particles/μm^2; $n = 90$). Earlier studies have reported that TMN neurons are GABAergic (Vincent et al., 1983; Ericson et al., 1991b), but the post-embedding method for electron microscopic immunocytochemistry is considerably less sensitive than pre-embedding methods that were used previously, and our animals were not treated with colchicine. Hence the density of gold particles over VLPO terminals was ~13 times as great as that over TMN dendrites ($p < 0.000001$; Kolmogorov–Smirnov test).

Retrograde tracing plus immunocytochemistry for GAD or galanin

Because of the presence of clusters of both GABAergic and galaninergic neurons in the VLPO area, and the known relationship of GABAergic and galaninergic terminals to TMN neurons, we examined a series of 11 additional cases in which retrograde labeling from the TMN was combined with immunocytochemistry for GAD or galanin. In four of these, the quality of both the retrograde transport and the immunocytochemistry was adequate to allow a semiquantitative analysis of the neurotransmitter content of VLPO neurons that projected to the TMNv. In each case, the injection site included the core of the TMNv but extended beyond this region. Hence the specificity of the projection for the TMNv was based on the observation above that VLPO neurons are only retrogradely labeled when injections into the posterolateral hypothalamus include the TMNv, and that the descending VLPO axons have a high specificity for TMN neurons.

In these four cases, we found that roughly 80% of all retrogradely labeled VLPO neurons contained GAD-ir and a similar number contained galanin-ir (Table 2, Fig. 6*e–g*). Regions outside the VLPO, particularly the dorsal portion of the lateral preoptic area and the ventromedial preoptic area, also contained several double-labeled neurons, although they were scattered among a majority of other neurons containing only one label. No specific staining was obtained in tissue that was incubated in preabsorbed primary antibody for either GAD or galanin.

Preoptic sections containing the VLPO were stained immunofluorescently for both GAD-ir and galanin-ir in three cases. These experiments demonstrated that GAD-immunoreactive neurons were abundant in cell groups throughout the rostral hypothalamus and adjacent basal forebrain (Mugnaini and Oertel, 1985), whereas the distribution of galanin-immunoreactive neurons was more restricted. Within the VLPO, almost every neuron found to contain galanin-ir was also found to contain GAD-ir (Fig. 6*h–j*). Several double-labeled neurons were found in regions outside the VLPO, including the dorsal portion of the lateral preoptic area and the ventromedial preoptic area, although they were scattered among a majority of other neurons containing only one label. Intensely single-labeled neurons were found in the same sections in areas other than the VLPO, such as the cortex, reticular thalamic nucleus, and lateral preoptic area (GAD-ir; Fig. 6, compare *i*,*j*) and the supraoptic nucleus (galanin-ir; Fig. 6, compare *h*,*j*), so that that the double-staining of VLPO neurons could not have represented a cross-reactivity of the antisera. As further controls, when either the GAD or galanin antiserum was omitted or replaced with normal rabbit serum, no specific staining was seen. In addition, in the double immunocytochemistry experiment, when the second primary antiserum in each sequence was omitted or substituted with normal rabbit serum, staining only for the first primary antiserum was seen.

DISCUSSION

Our observations demonstrate a massive and selective input from a small group of neurons in the ventral portion of the lateral preoptic area to the major cluster of histaminergic neurons in the brain, the TMNv. Electron microscopic observations confirm that the VLPO axon terminals form symmetric synapses onto TMNv proximal dendrites and cell bodies. Our results further hint that this is a topographically organized projection, with additional input primarily to the TMNm and TMNd from the medial preoptic area and to the TMNv from the dorsal lateral preoptic area. Approximately 70–80% of the cells that provide this projection contain both GABA and galanin, suggesting that they are inhibitory in nature. Furthermore, descending axons from the VLPO innervate the other monoaminergic cell groups in the brainstem that provide diffuse cortical projections, including the dopaminergic ventral tegmental area, the serotoninergic dorsal and median raphe nuclei, and the noradrenergic locus coeruleus. Hence, the VLPO is ideally situated to hyperpolarize simultaneously the monoaminergic components of the ascending arousal system. Because many VLPO neurons that project to the TMN are sleep active (Sherin et al., 1996), these observations support the hypothesis that the VLPO may play an important role in the regulation of wake–sleep states.

Technical considerations

We used a combination of retrograde and anterograde tracer experiments to define the VLPO projections more definitively than either approach can alone. Iontophoretic injections of retrograde tracers that are confined to the TMNv (case J-13) may be too small to label all of its afferents, whereas large injections necessarily include surrounding tissue, and retrogradely labeled cells may not project to the TMN. However, our anterograde transport experiments confirm that the TMNv is filled with anterogradely labeled fibers and boutons that appose TMN cell bodies and proximal dendrites only when the injection sites hit the VLPO.

TMN neurons may receive other types of afferents on their distal dendrites, which can extend for a considerable distance outside the borders of the nucleus. However, the inputs to their cell bodies are confirmed by our electron microscopic findings to be predominantly GABAergic. These VLPO terminals would be in an excellent position to hyperpolarize the TMN neurons, as confirmed by the demonstration that electrical stimulation of preoptic inputs to the TMN results in inhibitory postsynaptic potentials that are abolished by $GABA_A$ antagonists (Yang and Hatton, 1994).

Our double-labeling results indicate that nearly all of the gala-

Table 2. Summary of retrograde transport–immunocytochemical double labeling

		Number of labeled neurons in VLPO			
		GAD series		GAL series	
Case	Tracer	Retro	Retro + GAD	Retro	Retro + GAL
J-78c	CTB-gold	59	46	47	39
J-85c	CTB-gold	34	26		
J-85f	Fast blue	43	33	46	38
J-88d	Diamidino yellow	27	20	24	19
Total		163	125	117	96
% Double-labeled neurons		GAD	77%	GAL	82%

GAD, Glutamic acid decarboxylase; GAL, galanin; Retro, retrogradely labeled; VLPO, ventrolateral preoptic area.

ninergic VLPO cells that project to the TMN also are GABAergic. Although we used two rabbit antisera for this colocalization, replacing either primary antiserum with nonimmune serum abolished the double-labeling, indicating that it was not caused by cross-reactivity of the secondary antibodies. In addition, there were many single-labeled neurons of each type, confirming antibody specificity.

Visualization of GAD or galanin in retrogradely labeled VLPO neurons required that the animals be treated with colchicine. However, GABAergic and galaninergic terminals are found in the core of the TMNv in untreated rats, confirming that GABA and galanin are not induced in this system as an artifact of colchicine treatment (Cortes et al., 1990). Because colchicine treatment induces artifactual Fos staining, we could not demonstrate directly that the GABA/galanin cells in the VLPO that project to the TMN are also sleep active (Sherin et al., 1996). However, >50% of VLPO cells that are retrogradely labeled from the TMNv also express Fos protein during sleep, indicating that there is likely to be a large overlap. Studies using three distinct labels, such as combining *in situ* hybridization for neurotransmitter localization with retrograde transport and Fos staining, will be necessary to demonstrate these relationships definitively.

VLPO as a source of afferent input to the TMN

Although the efferent projections of the TMN and its role in behavioral state regulation have been extensively studied in various species (Panula et al., 1989; Schwartz et al., 1991; Onodera et al., 1993), only one systematic study of its afferent innervation using retrograde tracing has been published (Ericson et al., 1991a). In that study, Ericson and colleagues identified >70 cell groups in the rat brain (predominantly in the limbic forebrain) that were labeled after injection of retrograde tracer into the TMN region. However, anterograde tracer injections into many of these retrogradely labeled cell groups produced relatively modest numbers of fibers that entered the cell-dense core of the TMN (Conrad and Pfaff, 1976; Swanson, 1976; Wouterlood et al., 1987, 1988; Wouterlood and Gaykema, 1988; Ericson et al., 1991a; Wouterlood and Tuinhof, 1992; Gritti et al., 1994). The majority of anterogradely labeled fibers from these sites projected to targets medial, dorsal, or rostral to the TMN.

Our experiments agree with this previous work. Large injections of retrograde tracers demonstrated widespread labeling of neurons in limbic forebrain structures. However, by the use of strategically placed small injections of retrograde tracer into and around the cell-dense core of the TMNv, we were able to determine that VLPO inputs are concentrated in the TMNv. This observation was supported by our anterograde transport results, which also confirmed that the regions around the VLPO mainly target structures outside the TMN core.

VLPO as a source of afferents to other components of the ascending arousal system

Other VLPO efferents in our experiments targeted nearly all of the components of the ascending arousal system (for review, see Saper, 1987). Of particular interest were the inputs that we traced from the VLPO to other monoaminergic cell groups that, like the TMN, have wake-dependent activity and provide diffuse cortical innervation, including the serotoninergic dorsal and median raphe nuclei and the noradrenergic locus coeruleus (Aston-Jones and Bloom, 1981; Trulson et al., 1981).

The projection from the VLPO to the locus coeruleus has been reported previously, using a strategy similar to the one that we used (Luppi et al., 1995). Although the locus coeruleus region receives afferent input from >50 brain areas (Sakai et al., 1977; Cedarbaum and Aghajanian, 1978), selective examination of afferents to the cell-dense core of the locus coeruleus with discretely placed retrograde neuronal tracer reveals a much more restricted set of inputs (Aston-Jones et al., 1986; Luppi et al., 1995). We confirm with our anterograde tracer experiments that afferents from the VLPO ramify within the locus coeruleus core, giving off numerous boutons that are apposed to noradrenergic neurons.

In the dorsal and median raphe nuclei, many labeled afferent terminals also are apposed to serotoninergic neurons. However, a large percentage did not directly appose serotonin-immunolabeled cellular elements. This may have been caused by incomplete labeling of serotoninergic dendrites by the antiserum we used, but VLPO afferents may also contact other cell types in the raphe nuclei [and not all of the ascending diffuse projections from the dorsal raphe nucleus originate from serotoninergic neurons (for review, see Saper, 1987)].

In the basal forebrain and mesopontine cholinergic nuclei and the lateral hypothalamic MCH cell group, all of which provide diffuse ascending projections, the anterogradely labeled VLPO terminals seemed to avoid cholinergic and MCH-stained neurons, suggesting that they may innervate interneurons. The role of the VLPO in regulating the different components of the ascending arousal system will require careful electron microscopic studies of the patterns of innervation in these cell groups. However, the VLPO seems uniquely placed as a potential source of afferent influence to virtually all components of the ascending arousal system.

VLPO as a potential regulator of wake–sleep states

The region of the preoptic area containing the VLPO may play a critical role in inducing sleep. Lesions in this area cause insomnia, whereas electrical or chemical stimulation causes sleep (Sterman and Clemente, 1962; McGinty and Sterman, 1968; Szymusiak and McGinty, 1986; Sallanon et al., 1989; John et al., 1994). Nauta (1946) proposed a simple mechanism by which sleep-promoting neurons in the preoptic area would inhibit wake-promoting neurons in the posterior hypothalamus to produce sleep.

Our results are remarkably consistent with this model. We found previously that >50% of the VLPO neurons that project to the TMN are sleep active, as demonstrated by Fos-immunoreactivity (Sherin et al., 1996). The VLPO provides an intense and specific GABAergic and galaninergic set of inputs to the cell bodies and proximal dendrites of the histaminergic tuberomammillary nucleus in the posterior hypothalamus. Furthermore, the VLPO provides inputs to the serotoninergic dorsal and median raphe nuclei and to the noradrenergic locus coeruleus. All three of these monoaminergic populations are known to fire more slowly during slow wave sleep and to cease firing during REM sleep. The VLPO is an attractive candidate for simultaneously hyperpolarizing neurons in all three populations of monoaminergic neurons during sleep.

Finally, the relationship of VLPO terminals to interneurons in the cholinergic and MCH-immunoreactive systems of diffuse projection neurons is intriguing. These findings suggest that the VLPO neurons may play a key role in the function of a wide range of cell groups that contribute to the wakeful state. Further study of the relationship of descending VLPO inputs to the function of these cell groups is likely to provide important insights into the mechanisms for regulation of the wake–sleep state.

REFERENCES

Aston-Jones G, Bloom FE (1981) Activity of norepinephrine containing locus coeruleus neurons in behaving rats anticipates fluctuations in the sleep-waking cycle. J Neurosci 1:876–886.

Aston-Jones G, Ennis M, Pieribone VA, Nickell WT, Shipley MT (1986) The brain nucleus locus coeruleus. Afferent control of a broad efferent network. Science 234:734–737.

Bittencourt JC, Presse F, Arias C, Peto C, Vaughan J, Nahon JL, Vale W, Sawchenko PE (1992) The melanin-concentrating hormone system of the rat brain. An immunocytochemical and hybridization histochemical characterization. J Comp Neurol 319:218–245.

Bleier R, Cohn P, Siggelkow IR (1979) A cytoarchitectonic atlas of the hypothalamus and hypothalamic third ventricle of the rat. Anatomy of the hypothalamus. In: Handbook of the hypothalamus, Vol 1 (Morgane PJ, Panksepp J, eds), pp 137–220. New York: Marcel Dekker.

Cedarbaum JM, Aghajanian GK (1978) Afferent projections to the rat locus coeruleus as determined by a retrograde tracing technique. J Comp Neurol 178:1–16.

Chiba T, Murata Y (1985) Afferent and efferent connections of the medial preoptic area in the rat: A WGA-HRP study. Brain Res Bull 14:261–272.

Conrad LCA, Pfaff DW (1976) Efferents from medial basal forebrain and hypothalamus in the rat. I. An autoradiographic study of the medial preoptic area. J Comp Neurol 169:185–220.

Cortes R, Ceccatelli S, Schalling M, Hokfelt T (1990) Differential effects of intercerebroventricular colchicine administration of the expression of mRNAs for neuropeptides and neurotransmitter enzymes with special emphasis on galanin: an in situ hybridization study. Synapse 6:369–391.

de Lacalle S, Lim C, Sobreviela T, Mufson EJ, Hersh LB, Saper CB (1994) Cholinergic innervation in the human hippocampal formation including the entorhinal cortex. J Comp Neurol 345:321–344.

Elmquist JK, Saper CB (1996) Activation of neurons projecting to the paraventricular nucleus of the hypothalamus by intravenous lipopolysaccharide. J Comp Neurol 374:315–331.

Elmquist JK, Fox CA, Ross LR, Jacobson CD (1992) Galanin-like immunoreactivity in the adult and developing Brazilian opossum brain. Dev Brain Res 67:161–179.

Elmquist JK, Scammell TE, Jacobson CD, Saper CB (1996) Distribution of Fos-like immunoreactivity in the rat brain following intravenous lipopolysaccharide administration. J Comp Neurol 371:85–103.

Ericson H, Watanabe T, Kohler C (1987) Morphological analysis of the tuberomammillary nucleus in the rat brain: delineation of subgroups with antibody against L-histidine decarboxylase as a marker. J Comp Neurol 263:1–24.

Ericson H, Blomqvist A, Kohler C (1991a) Origin of neuronal inputs to the region of the tuberomammillary nucleus of the rat brain. J Comp Neurol 311:45–64.

Ericson HC, Kohler C, Blomqvist A (1991b) GABA-like immunoreactivity in the tuberomammillary nucleus: an electron microscopic study in the rat. J Comp Neurol 305:462–469.

Gritti I, Mainville L, Jones BE (1994) Projections of GABAergic and cholinergic basal forebrain and GABAergic preoptic-anterior hypothalamic neurons to the posterior lateral hypothalamus of the rat. J Comp Neurol 339:251–268.

Grove EA (1988) Efferent connections of the substantia innominata. J Comp Neurol 277:347–364.

Hallanger A, Levey AI, Lee HJ, Rye DB, Wainer BH (1987) The origins of cholinergic and other subcortical afferents to the thalamus in the rat. J Comp Neurol 262:105–124.

Hayaishi H, Takagi H, Takeda Y, Kubota M, Tohyama M, Watanabe T, Wada H (1984) Fine structure of histaminergic neurons in the caudal magnocellular nucleus of the rat as demonstrated by immunohistochemistry using histidine decarboxylase as a marker. J Comp Neurol 229:233–241.

Herbert H, Saper CB (1990) Cholecystokinin-, galanin-, and corticotropin-releasing factor-like immunoreactive projections from the nucleus of the solitary tract to the parabrachial nucleus in the rat. J Comp Neurol 293:581–598.

Itowi N, Yamatodani A, Kiyono S, Hiraiwa ML, Wada H (1991) Effect of histamine depletion on the circadian amplitude of the sleep-wakefulness cycle. Physiol Behav 49:643–646.

John J, Kumar VM, Gopinath G, Ramesh V, Mallick H (1994) Changes in sleep-wakefulness after kainic acid lesion of the preoptic area in rats. Jpn J Physiol 44:231–242.

Kalivas PW (1982) Histamine-induced arousal in the conscious and pentobarbital-pretreated rat. J Pharmacol Exp Ther 222:37–42.

Kiyono S, Seo ML, Shibagaki M, Watanabe T, Maeyama K, Wada H (1985) Effects of alpha-fluoromethylhistidine on sleep-waking parameters in rats. Physiol Behav 34:615–617.

Kohler C, Ericson H, Watanabe T, Polak J, Palay SL, Palay V, Chan-Palay V (1986) Galanin immunoreactivity in hypothalamic histamine neurons: further evidence for multiple chemical messengers in the tuberomammillary nucleus. J Comp Neurol 250:58–64.

Lin JS, Sakai K, Jouvet M (1986) Role of hypothalamic histaminergic systems in the regulation of states of vigilance in the cat. C R Acad Science III 303:469–474.

Lin JS, Sakai K, Jouvet M (1988) Evidence for histaminergic arousal mechanisms in the hypothalamus of cats. Neuropharmacology 27:111–122.

Lin JS, Sakai K, Vanni-Mercier G, Jouvet M (1989) A critical role for the posterior hypothalamus in the mechanisms of wakefulness determined by microinjection of muscimol in freely moving cats. Brain Res 479:225–240.

Lin JS, Sakai K, Vanni-Mercier G, Arrang JM, Garbarg M, Schwartz JC, Jouvet M (1990) Involvement of histaminergic neurons in arousal mechanisms demonstrated with H3-receptor ligands in the cat. Brain Res 523:325–330.

Lin JS, Sakai K, Vanni-Mercier G, Jouvet M (1994) Hypothalamopreoptic histaminergic projections in sleep-wake control in the cat. Eur J Neurosci 66:618–625.

Lin JS, Hou Y, Sakai K, Jouvet J (1996) Histaminergic descending inputs to the mesopontine tegmentum and their role in the control of cortical activation and wakefulness in the cat. J Neurosci 16:1523–1537.

Lindsley DB, JW Bowden, Magoun HW (1949) Effect upon the EEG of acute injury to the brain stem activating system. Electroencephalogr Clin Neurophysiol 1:475.

Llewellyn-Smith IJ, Minson JB, Wright AP, Hodgson AJ (1990) Cholera toxin B-gold, a retrograde tracer that can be used in light and electron microscopic immunocytochemical studies. J Comp Neurol 294:179–191.

Luppi PH, Aston-Jones, Akaoka H, Chouvet G, Jouvet M (1995) Afferent projections to the rat locus coeruleus demonstrated by retrograde and anterograde tracing with cholera-toxin B subunit and PHA-L. Neuroscience 65:119–160.

McGinty DJ, Sterman MB (1968) Sleep suppression after basal forebrain lesions in the cat. Science 160:1253–1255.

Meibach RC, Siegel A (1977) Efferent connections of the septal area in the rat: an analysis utilizing retrograde and anterograde transport methods. Brain Res 119:1–20.

Melander T, Hökfelt T, Rökeaus Ä (1986) Distribution of galanin-like immunoreactivity in the rat central nervous system. J Comp Neurol 248:475–517.

Merighi A, Polak JM (1993) Post-embedding immunogold staining. In: Immunohistochemistry II. IBRO Handbook Series: Methods in the neurosciences, Vol 14 (Cuello AC, ed), pp 229–264. Chichester, UK: Wiley.

Moga MM, Saper CB (1994) Neuropeptide-immunoreactive neurons projecting to the paraventricular hypothalamic nucleus in the rat. J Comp Neurol 346:137–150.

Moga MM, Saper CB, Gray TS (1989) The bed nucleus of the stria terminalis: cytoarchitecture, immunohistochemistry and projection to the parabrachial nucleus in the rat. J Comp Neurol 283:315–332.

Monnier M, Sauer R, Hatt AM (1970) The activating effect of histamine on the central nervous system. Int Rev Neurobiol 12:265–305.

Monti JM (1993) Involvement of histamine in the control of the waking state. Life Sci 53:1331–1338.

Monti JM, Pellejero T, Jantos H (1986) Effects of H_1 and H_2 histamine receptor antagonists on sleep and wakefulness in the rat. J Neural Transm 66:1–11.

Monti JM, D'Angelo L, Jantos H, Pazos S (1988) Effects of alpha-fluoromethylhistidine on sleep and wakefulness in the rat. J Neural Transm 72:141–145.

Monti JM, Jantos H, Boussard M, Altier H, Orellana C, Olivera S (1991) Effects of selective activation or blockade of the histamine H3 receptor on sleep and wakefulness. Eur J Pharmacol 205:283–287.

Mugnaini E, Oertel WH (1985) An atlas of the distribution of GABAergic neurons and terminals in the rat CNS as revealed by GAD immunohistochemistry. In: Handbook of chemical neuroanatomy, Vol 4, GABA and neuropeptides in the CNS: Part 1 (Bjorklund A, Hokfelt T, eds), pp 436–608. Amsterdam: Elsevier.

Nauta WJH (1946) Hypothalamic regulation of sleep in rats. An experimental study. J Neurophysiol 9:285–316.

Nicholson AN, Pascoe PA, Stone BM (1985) Histaminergic systems and sleep: studies in man with H1 and H2 antagonists. Neuropharmacology 24:245–250.

Nitz D, Siegel JM (1996) GABA release in posterior hypothalamus across sleep-wake cycle. Am J Physiol 271:R1707–R1712.

Onodera K, Yamatodani A, Watanabe T, Wada H (1993) Neuropharmacology of the histaminergic neuron system in the brain and its relationship with behavioral disorders. Prog Neurobiol 42:685–702.

Panula P, Pirvola U, Auvinen S, Airaksinen MS (1989) Histamine-immunoreactive nerve fibers in the rat brain. Neuroscience 28:585–610.

Pieribone VA, Aston-Jones G (1988) The iontophoretic application of flouro-gold for the study of afferents to deep brain nuclei. Brain Res 475:259–271.

Pieribone VA, Xu ZQ, Zhang X, Grillner S, Bartfai T, Hokfelt T (1995) Galanin induces a hyperpolarization of norepinephrine-containing locus coeruleus neurons in the brainstem slice. Neuroscience 64:861–874.

Reiner PB, McGeer EG (1987) Electrophysiological properties of cortically projecting histamine neurons of the rat hypothalamus. Neurosci Lett 73:43–47.

Risold PY, Canteras NS, Swanson LE (1994) Origin of projections from the anterior hypothalamic nucleus: a PHA-L study in the rat. J Comp Neurol 348:1–40.

Rizvi TA, Murphy AZ, Ennis M, Behbehani MM, Shipley MT (1995) Medial preoptic area afferents to periaqueductal gray medullo-output neurons: a combined fos and tract tracing study. J Neurosci 16:333–344.

Sakai K, Touret M, Salver D, Leger L, Jouvet M (1977) Afferent projections to the cat locus coeruleus as visualized by the horseradish peroxidase technique. Brain Res 119:21–41.

Sallanon M, Sakai M, Buda C, Puymartin M, Jouvet M (1988) Increase of paradoxical sleep induced by microinjections of ibotenic acid into the ventrolateral part of the posterior hypothalamus in the cat. Arch Ital Biol 126:87–97.

Sallanon M, Denoyer M, Kitahama K, Aubert C, Gay N, Jouvet M (1989) Long-lasting insomnia induced by preoptic neuron lesions and its transient reversal by muscimol injection into the posterior hypothalamus in the cat. Neuroscience 32:669–683.

Saper CB (1987) Diffuse cortical projection systems: anatomical organization and role in cortical function. In: Handbook of physiology. The nervous system V. (Plum F, ed), pp 169–210. Bethesda, MD: American Physiological Society.

Saper CB, Swanson LW, Cowan WM (1978) The efferent connections of the anterior hypothalamic area of the rat, cat and monkey. J Comp Neurol 182:575–600.

Saper CB, Akil H, Watson SJ (1986) Lateral hypothalamic innervation of the cerebral cortex: immunoreactive staining for a peptide resembling but immunochemically distinct from pituitary/arcuate α-melanocyte stimulating hormone. Brain Res Bull 16:107–120.

Schonrock B, Busselberg D, Haas HL (1991) Properties of tuberomammillary histamine neurones and their response to galanin. Agents Actions 33:135–137.

Schwartz J, Arrang JM, Garbarg M, Pollard H, Ruat M (1991) Histaminergic transmission in the mammalian brain. Physiol Rev 71:1–51.

Semba K, Reiner P, McGeer EG, Fibiger H (1989) Brainstem projecting neurons in the rat basal forebrain: neurochemical, topographical, and physiological distinctions from cortically projecting cholinergic neurons. Brain Res Bull 22:501–509.

Senba E, Daddona PE, Watanabe T, Wu JY, Nagy JI (1985) Coexistence of adenosine deaminase, histidine decarboxylase, and glutamate decarboxylase in hypothalamic neurons of the rat. J Neurosci 5:3393–3402.

Seutin VP, Verbanck P, Massotte L, Dresse A (1989) Galanin decreases the activity of locus coeruleus neurons in vitro. Eur J Pharmacol 164:373–376.

Sherin JE, Shiromani PJ, McCarley RW, Saper CB (1996) Activation of ventrolateral preoptic neurons during sleep. Science 271:216–219.

Simerly RB, Swanson LW (1988) Projections of the medial preoptic nucleus: a *Phaseolus vulgaris* leucoagglutinin anterograde tract-tracing study in the rat. J Comp Neurol 270:209–241.

Simerly RB, Swanson LW, Gorski RA (1984) Demonstration of a sexual dimorphism in the distribution of serotonin-immunoreactive fibers in the medial preoptic nucleus of the rat. J Comp Neurol 225:151–166.

Simerly RB (1995) Anatomical substrates of hypothalamic integration. In: The rat nervous system (Paxinos G, ed), pp 353–376. San Diego: Academic.

Snyder SH, Brown B, Kuhar MJ (1974) The subsynaptosomal localization of histamine, histidine decarboxylase and histamine methyltransferase in rat hypothalamus. J Neurochem 23:37–45.

Steininger TL, Alam MN, Szymusiak R, McGinty D (1996) State-dependent discharge of neurons in the rat posterior hypothalamus. Soc Neurosci Abstr 22:689.

Steriade M (1988) New vistas on the morphology, chemical transmitters and physiological actions of the ascending brainstem reticular system. Arch Ital Biol 126:225–238.

Steriade M, McCormick DA, Sejnowski TJ (1993) Thalamocortical oscillations in the sleeping and aroused brain. Science 262:679–685.

Sterman MB, Clemente CD (1962) Forebrain inhibitory mechanisms: cortical synchronization induced by basal forebrain stimulation. Exp Neurol 6:91–102.

Sundstrom E, Melander T (1988) Effects of galanin on 5-HT neurons in the rat CNS. Eur J Pharmacol 146:327–329.

Swanson LW (1976) An autoradiographic study of the efferent connections of the preoptic region in the rat. J Comp Neurol 167:227–256.

Swanson LW, Cowan WM (1979) The connections of the septal region in the rat. J Comp Neurol 186:621–655.

Swanson LW, Mogenson GJ, Gerfen CR, Robinson P (1984) Evidence for a projection from the lateral preoptic area and substantia innominata to the mesencephalic locomotor region in the rat. Brain Res 295:161–178.

Swett CP, Hobson JA (1968) The effects of posterior hypothalamic lesions on behavioral and electrographic manifestations of sleep and waking in cats. Arch Ital Biol 106:283–293.

Szymusiak R, McGinty D (1986) Sleep suppression following kainic acid-induced lesions of the basal forebrain. Exp Neurol 94:598–614.

Tasaka K, Chung YH, Sawada K, Mio M (1989) Excitatory effect of histamine on the arousal system and its inhibition by H1 blockers. Brain Res Bull 22:271–275.

Tomimoto H, Kamo H, Kameyama M, McGeer PL, Kimura H (1987) Descending projections of the basal forebrain in the rat demonstrated

by the anterograde neural tracer *Phaseolus vulgaris* leucoagglutinin (PHA-L). Brain Res 425:248–255.

Trulson ME, Jacobs BL, Morrison AR (1981) Raphe unit activity during REM sleep in normal cats and in pontine lesioned cats displaying REM sleep without atonia. Brain Res 226:75–91.

Vanni-Mercier G, Sakai K, Jouvet M (1984) "Waking-state specific" neurons in the caudal hypothalamus of the cat. C R Acad Sci III 298:195–200.

Vincent SR, Hokfelt T, Skirboll LR, Wu J-Y (1983) Hypothalamic gamma-aminobutyric acid neurons project to the neocortex. Science 220:1309–1311.

Wada H, Inagaki N, Yamatodani A, Watanabe T (1991) Is the histaminergic neuron system a regulatory center for whole brain activity? Trends Neurosci 14: 415–418.

Watanabe T, Taguchi Y, Hayashi H, Tanaka J, Shiosaka S, Tohyama M, Kubota H, Terano Y, Wada H (1983) Evidence for the presence of a histaminergic neuron system in the rat brain; an immunocytochemical analysis. Neurosci Lett 39:249–254.

Watanabe T, Taguchi Y, Shiosaka S, Tanaka J, Kubota H, Terano Y, Tohyama M, Wada H (1984) Distribution of the histaminergic neuron system in the central nervous system of the rat: a fluorescent immunocytochemical analysis with histidine decarboxylase as a marker. Brain Res 295:13–25.

White JM, Rumbold GR (1988) Behavioral effect of histamine and its antagonists. A review. Psychopharmacology 1–14.

Wilcox BJ, Seybold VS (1982) Localization of neuronal histamine in rat brain. Neurosci Lett 29:105–110.

Wouterlood FG, Gaykema RPA (1988) Innervation of histaminergic neurons in the posterior hypothalamic region by medial preoptic neurons. Anterograde tracing with *Phaseolus vulgaris*-leucoagglutinin combined with immunocytochemistry of histidine decarboxylase in the rat. Brain Res 455:170–176.

Wouterlood FG, Tuinhof R (1992) Subicular efferents to histaminergic neurons in the posterior hypothalamic region of the rat studied with PHA-L tracing method combined with histidine decarboxylase immunocytochemistry. J Hirnforsch 33:451–465.

Wouterloud FG, Sauren YMHF, Steinbusch HWM (1986) Histaminergic neurons in the rat brain: correlative immunocytochemistry, Golgi impregnation, and electron microscopy. J Comp Neurol 252:227–244.

Wouterlood FG, Steinbusch HWM, Luiten PGM, Bol JGJM (1987) Projection from the prefrontal cortex to histaminergic cell groups in the posterior hypothalamic region of the rat. Anterograde tracing with *Phaseolus vulgaris*-leucoagglutinin combined with immunocytochemistry of histidine decarboxylase. Brain Res 406:330–336.

Wouterlood FG, Gaykema RPA, Steinbusch HWM, Watanabe T, Wada H (1988) The connections between the septum-diagonal band complex and histaminergic neurons in the posterior hypothalamus of the rat. Anterograde tracing with *Phaseolus vulgaris*-leucoagglutinin combined with immunocytochemistry of histidine decarboxylase. Neuroscience 26:827–845.

Yamamoto T, Ochi J, Daddona PE, Nagy JI (1990) Ultrastructural immunolocalization of adenosine deaminase in histaminergic neurons of the tuberomammillary nucleus of the rat. Brain Res 527:335–341.

Yang QZ, Hatton GI (1994) Excitatory and inhibitory inputs to histaminergic tuberomammillary nucleus neurons. Soc Neurosci Abstr 20:346.